

NASA Technical Memorandum

NASA TM - 86587

IGNITION OVERPRESSURE STUDY FROM SOLID ROCKET MOTOR FIRINGS

By Douglas D. Counter

Structures and Dynamics Laboratory
Science and Engineering Directorate

March 1987

(NASA-TM-86587) IGNITION OVERPRESSURE STUDY
FROM SOLID ROCKET MOTOR FIRINGS (NASA) 31 p
CSCL 21H

N87-18607

Unclas

G3/20 43792

NASA

National Aeronautics and
Space Administration

George C. Marshall Space Flight Center



1. REPORT NO. NASA TM-86587		2. GOVERNMENT ACCESSION NO.		3. RECIPIENT'S CATALOG NO.	
4. TITLE AND SUBTITLE Ignition Overpressure Study from Solid Rocket Motor Firings				5. REPORT DATE March 1987	
				6. PERFORMING ORGANIZATION CODE	
7. AUTHOR(S) Douglas D. Counter				8. PERFORMING ORGANIZATION REPORT #	
9. PERFORMING ORGANIZATION NAME AND ADDRESS George C. Marshall Space Flight Center Marshall Space Flight Center, Alabama 35812				10. WORK UNIT NO.	
				11. CONTRACT OR GRANT NO.	
				13. TYPE OF REPORT & PERIOD COVERED Technical Memorandum	
12. SPONSORING AGENCY NAME AND ADDRESS National Aeronautics and Space Administration Washington, D.C. 20546				14. SPONSORING AGENCY CODE	
15. SUPPLEMENTARY NOTES Prepared by Induced Environment Branch, Aerophysics Division, Structures and Dynamics Laboratory, Science and Engineering Directorate.					
16. ABSTRACT The objective of this study was to investigate, through experimental means, the basic mechanisms influencing ignition overpressure and to determine ways to suppress ignition overpressure. Ignition overpressure was studied using solid rocket motors with geometry scaled at 1 percent of the Shuttle's Solid Rocket Boosters. Both water injection and aerosol foam were examined as a means of reducing ignition overpressure. The results of the water injection tests indicate that a relatively small amount of water is sufficient to provide significant suppression. Of the flow rates tested, the lower water injection flow rates provided the best reduction of the ignition overpressure wave. Also, the test results show there is an optimum water flow rate range that provides the best suppression, and as this range is exceeded the effectiveness of water to reduce ignition overpressure is decreased. Aerosol foam provided very little reduction of ignition overpressure, but only small volumes of foam were used and further testing is necessary to determine its total effectiveness as a means of suppression.					
17. KEY WORDS Ignition Overpressure Suppression			18. DISTRIBUTION STATEMENT Unclassified - Unlimited		
19. SECURITY CLASSIF. (of this report) Unclassified		20. SECURITY CLASSIF. (of this page) Unclassified		21. NO. OF PAGES 30	22. PRICE NTIS



TABLE OF CONTENTS

	Page
INTRODUCTION	1
DESCRIPTION	8
CONCLUSIONS AND RECOMMENDATIONS.....	22
REFERENCES.....	24

PRECEDING PAGE BLANK NOT FILMED

LIST OF ILLUSTRATIONS

Figure	Title	Page
1.	Drawing of SRM nozzle	2
2.	Drawing of SRM assembly	3
3.	Test configuration for 1 percent SRM ignition overpressure	4
4.	1 percent SRM test configuration, top view	5
5.	1 percent SRM test configuration, bottom view	6
6.	Drawing of water manifold	7
7.	Typical chamber pressure time histories	9
8.	Overpressure versus chamber pressure rise rate	9
9.	Duct overpressure measurement K9 versus chamber pressure impulse	10
10.	Overpressure (K9) versus chamber pressure	12
11.	Overpressure (K9) versus chamber pressure peak	12
12.	Overpressure (K9) versus RSS P_c and P_c peak	13
13.	Overpressure (K11) versus RSS P_c and P_c peak	13
14.	Average duct overpressure (K2-K11) versus RSS of P_c and P_c peak	14
15.	Duct overpressure (dry) versus RSS P_c and P_c peak	14
16.	1 percent SRM ignition overpressure test (with and without water injection)	15
17.	Unnormalized duct overpressure versus downstream location	16
18.	Normalized pressure ratio versus downstream location	17
19.	Downstream location versus overpressure wave arrival time	18
20.	Normalized pressure ratio versus flow rate ratio	18

LIST OF ILLUSTRATIONS (Concluded)

Figure	Title	Page
21.	Average normalized pressure ratio versus flow rate ratio	20
22.	Exit pressure ratio (K11) versus flow rate ratio	20
23.	Pressure ratio for average vehicle measurements versus flow rate ratio (6.4 percent model tests)	21
24.	Pressure ratio versus downstream location (water injection system located at 0, 20, and 40 in. from nozzle exit plane).....	21
25.	Normalized pressure ratio versus distance downstream	22

LIST OF TABLES

Table	Title	Page
1.	Peak Overpressure Readings for Dry SRM Tests.....	8
2.	Peak Overpressure Readings for Wet SRM Tests	15

DEFINITION OF SYMBOLS

Symbol	Definition
P_c	Chamber pressure
$P_c \text{ peak}$	Chamber pressure peak
$\dot{\omega}_w/\dot{\omega}_p$	Flow rate ratio, water flow rate to propellant flow rate
$P_{\text{water}}/P_{\text{dry}}$	Pressure ratio, overpressure of water test to overpressure of dry test

NONSTANDARD ABBREVIATIONS

ETR	Eastern Test Range
IOP	Ignition overpressure
MSFC	Marshall Space Flight Center
RSS	Root sum squares
SRB	Solid Rocket Booster
SRM	Solid Rocket Motor
VAFB	Vandenberg Air Force Base

TECHNICAL MEMORANDUM

IGNITION OVERPRESSURE STUDY FROM SOLID ROCKET MOTOR FIRINGS

INTRODUCTION

The purpose of this project was to use experimental means to investigate the basic mechanisms influencing ignition overpressure, and to study methods of suppressing ignition overpressure. Both water injection at various flow rates and aerosol foam were tested as a means of reducing ignition overpressure.

Pressure waves propagate from rocket nozzles when solid propellant ignition begins. Generally, these pressure waves then become quite critical in inducing loads on aerospace vehicles and launch structures with large surface areas. It is important to develop means of predicting these pressures and ultimately learn how to control them via design of operational limitations. Also, data and mathematical models are needed to describe the basic phenomena as launch vehicles evolve to advanced vehicle configurations. Advanced vehicles will require greater emphasis on overpressure suppression techniques to keep pace with the more stringent requirements due to more sensitive payloads and to increased overpressure source strengths. Therefore, it is important to develop a means of prediction, both analytical and empirical methods, which can provide guidelines for overpressure definition and control.

The physical mechanisms that suppress ignition overpressure are not exactly understood. It is likely that the water, through complex transport processes such as momentum, heat, and mass transfer, is able to cool the hot mass of gases from the exhaust which drive the overpressure wave. It is also likely that this wave is further attenuated to some degree as it propagates through the complex mixtures of exhaust gases, steam, and water droplets [1].

The Solid Rocket Motor (SRM) firings used for this study were conducted at NASA Test Laboratory test stand 116 at MSFC. Solid propellant rocket motors with geometry scaled at 1 percent of the Shuttle's Solid Rocket Boosters were utilized with variable chamber pressure and chamber pressure rise rates to provide an ignition overpressure (IOP) source. The SRMs are 2 in. in diameter and 4 in. long. Drawings of the SRM nozzle and motor assembly are shown in Figures 1 and 2. The SRM has a burn time of approximately 700 to 800 msec. The SRMs were fired into a simple cylindrical duct 10 ft long. The IOP was measured with pressure transducers in the duct located at 6, 9, 12, 18, 24, 30, 36, 48, 60, and 120 in. from the nozzle exit plane. The pressure transducers used in the tests were Kulite overpressure gauges. The test configuration and the location of the pressure transducers are shown in Figure 3. Figures 4 and 5 show the mounting of the SRM on the test stand and the mounting of the pressure transducers along the duct. The motors were fired vertically into the duct, which causes the exhaust gases to behave in a one-dimensional piston-like motion so that the overpressure wave is generated. The first tests (dry flows) were used to obtain a baseline for the test configuration and to determine the controlling factors in ignition overpressure. The next series of tests were used to study the effect of water injection on IOP and to determine the relationship between overpressure suppression and water flow rate. The water injection system consisted of

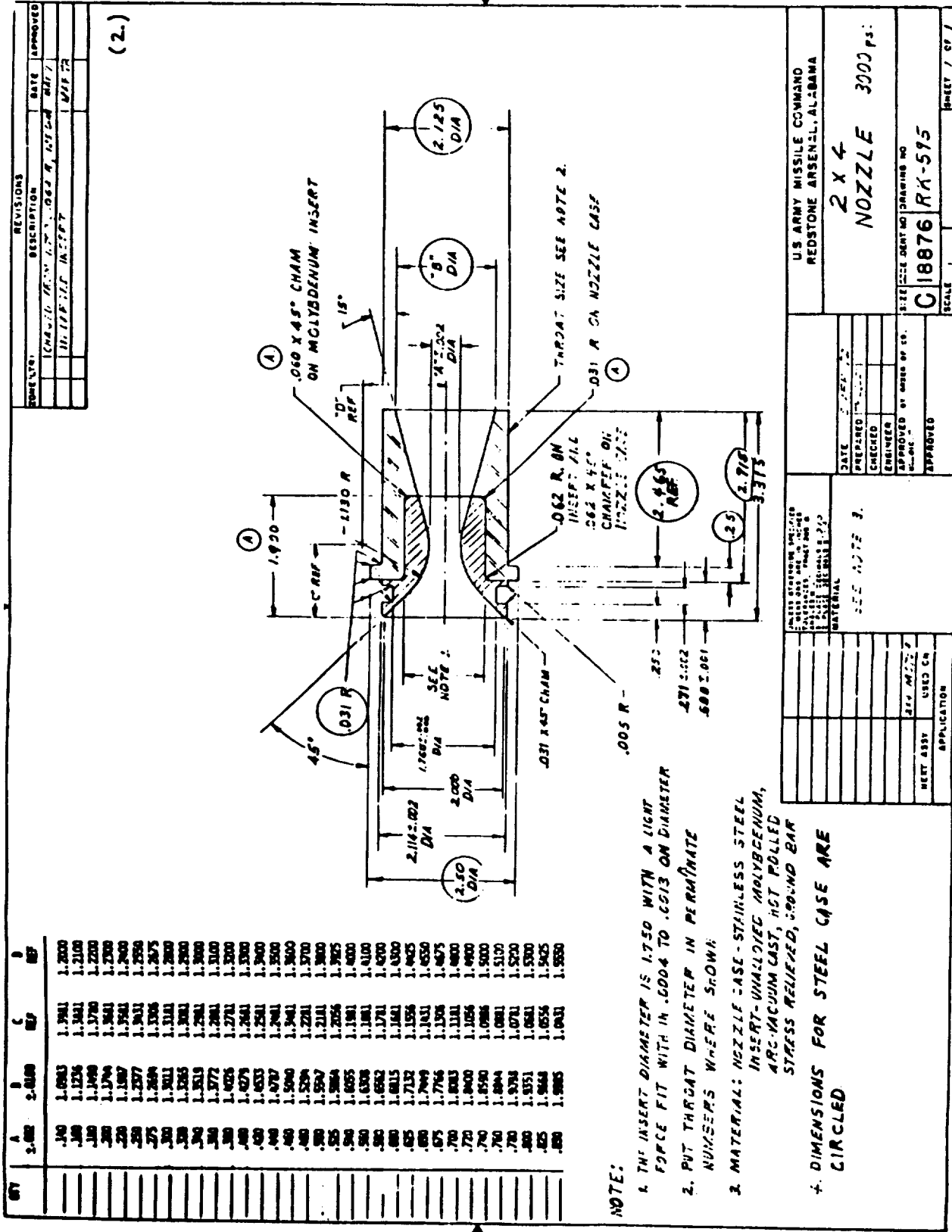
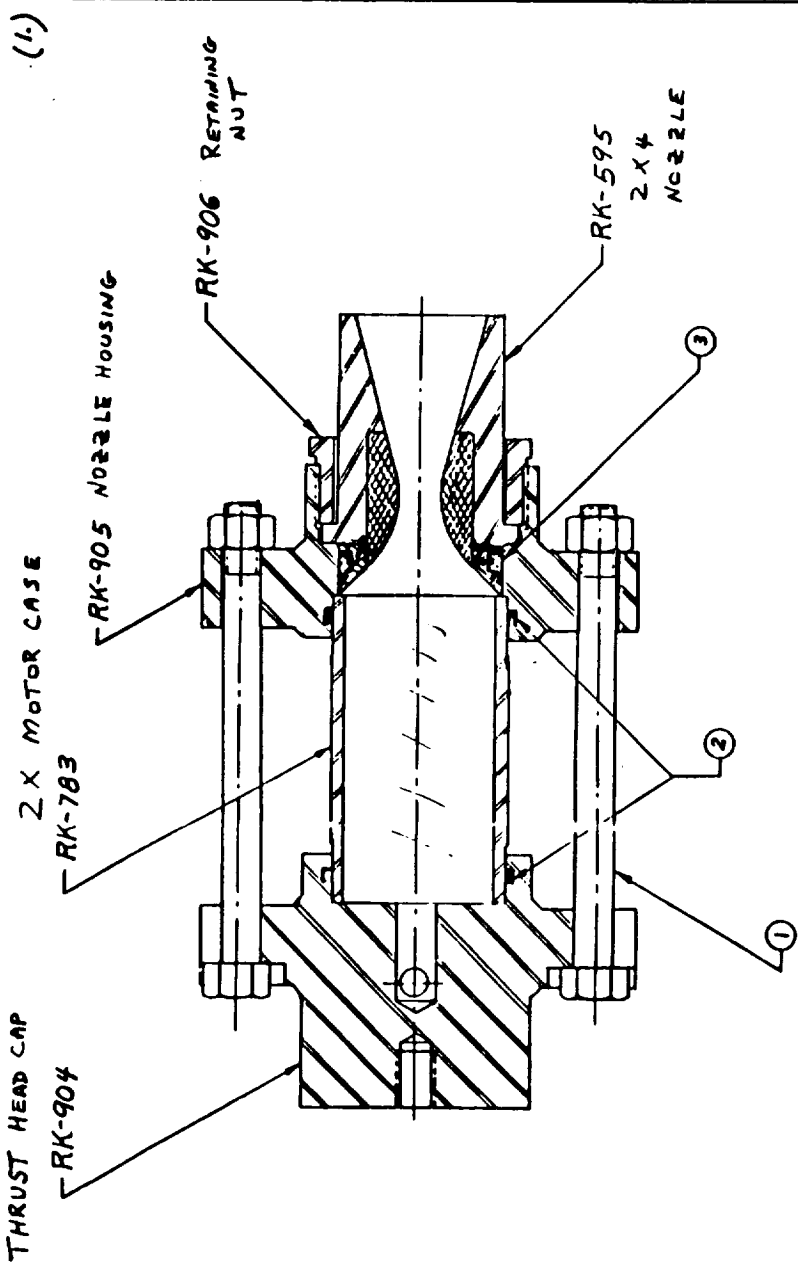


Figure 1. Drawing of SRM nozzle.

REVISION	DESCRIPTION	DATE	APPROVED



ORIGINAL PAGE IS
OF POOR QUALITY

U.S. ARMY MISSILE COMMAND REDSTONE ARSENAL, ALABAMA		2 X 4 MOTOR ASSEMBLY 3000 P.S.I.		SHEET 1 OF 1
DATE: 7 MAR 75 PREPARED BY: [blank] CHECKED: [blank] ENGINEER: [blank] APPROVED BY: [blank]		SIZE: [blank] CENT NO: [blank] DRAWING NO: C18876 PART NO: RK-903		SCALE: [blank]
THIS DRAWING IS UNCLASSIFIED EXCEPT WHERE SHOWN OTHERWISE		APPLICATION: [blank]		
PART NO 1 2 3 4 5	RETAINING NUT NOZZLE HOUSING THRUST HEAD CAP 2 X MOTOR CASE 2 X NOZZLE O-RING NO. 2-325 MATERIAL: BUNA-N O-RING NO. 2-223 MATERIAL: BUNA-N O-RING NO. 2-223 MATERIAL: BUNA-N	QTY/ASBY 1 1 1 1 1 2 2	NET ASBY [blank] [blank] [blank] [blank] [blank] [blank] [blank]	USED ON [blank] [blank] [blank] [blank] [blank] [blank] [blank]
DESCRIPTION				

Figure 2. Drawing of SRM assembly.

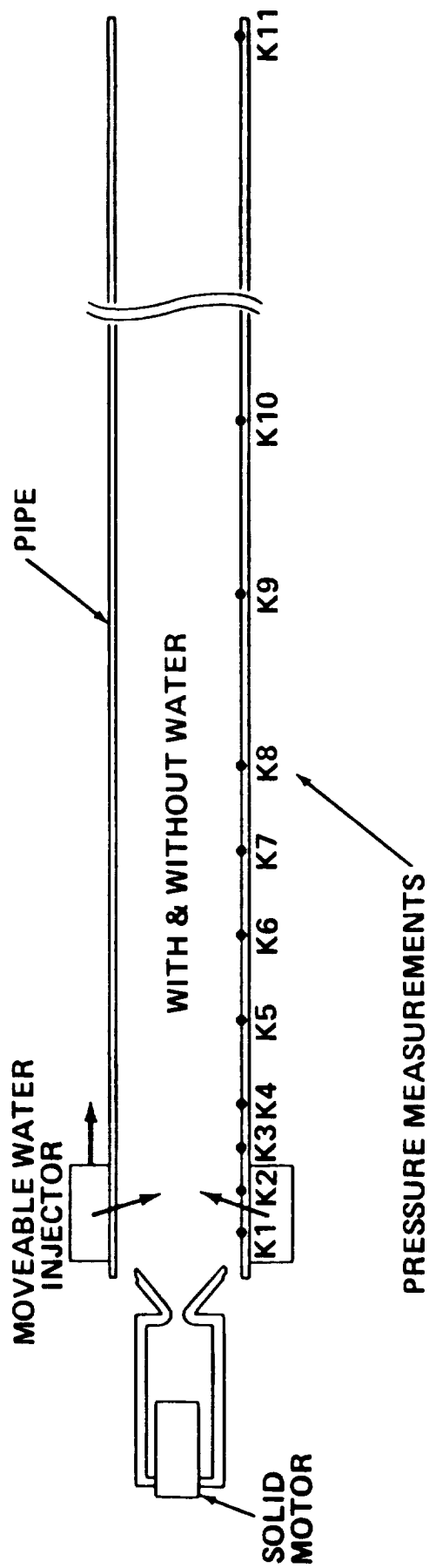


Figure 3. Test configuration for 1 percent SRM ignition overpressure.

ORIGINAL PAGE IS
OF POOR QUALITY

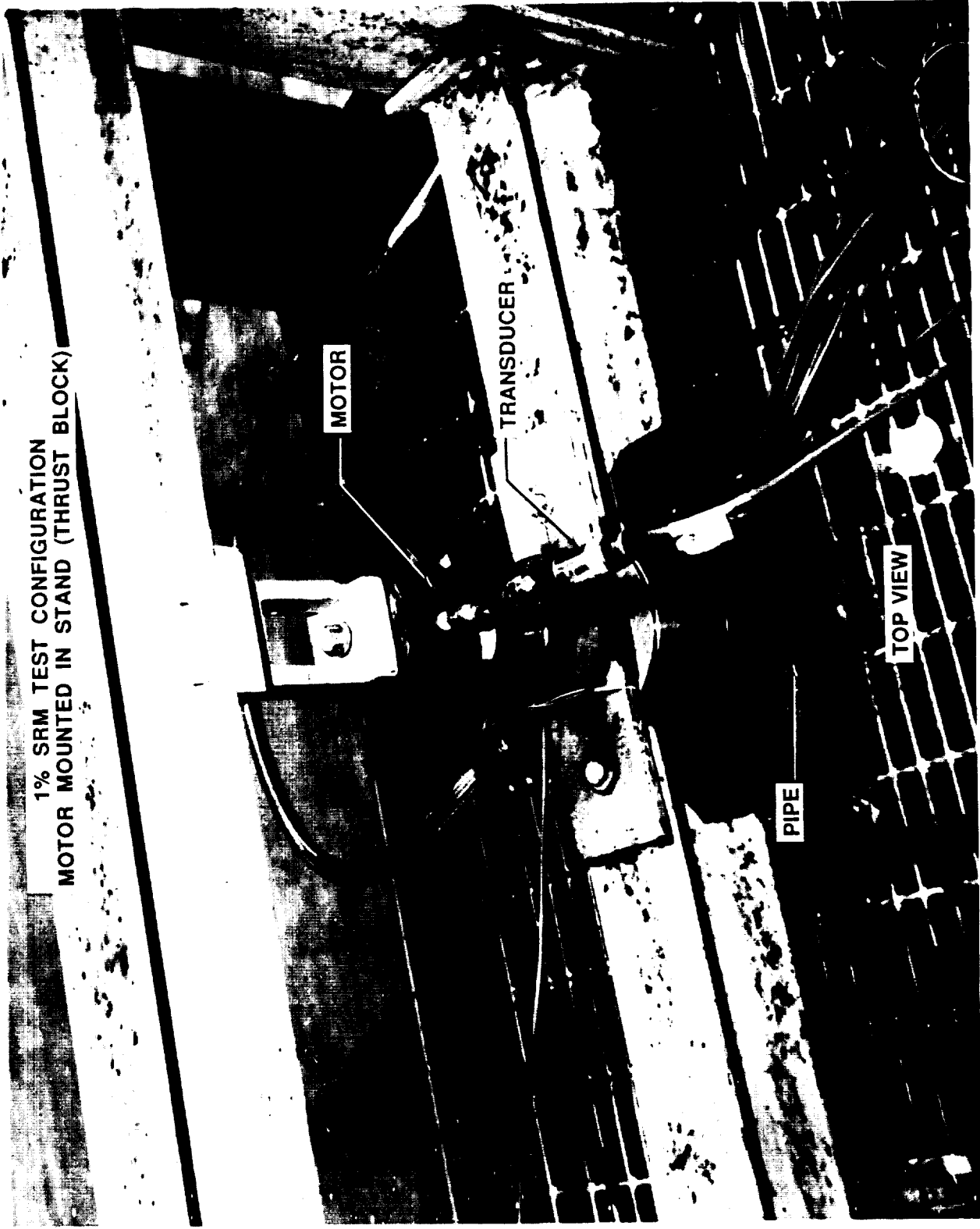


Figure 4. 1 percent SRM test configuration, top view.

ORIGINAL PAGE IS
OF POOR QUALITY



Figure 5. 1 percent SRM test configuration, bottom view.

jackets mounted on the pipe located at the nozzle exit plane. The water manifold used in the water flow tests is shown in Figure 6. The water was injected across the pipe at the desired water flow rate using a nozzle with a diameter of 7/16 in. Water injection tests were conducted using a water flow rate to propellant rate ($\dot{\omega}_w/\dot{\omega}_p$) of 0.075, 0.15, 0.225, 0.3, 0.45, 0.6, 0.75, and 0.9. To study the effect of changing the location of the water injection system, SRM firings were conducted with the water injection system located at 20 and 40 in. from the nozzle exit. Also, aerosol foam tests were conducted to determine how effective foam was at reducing the IOP.

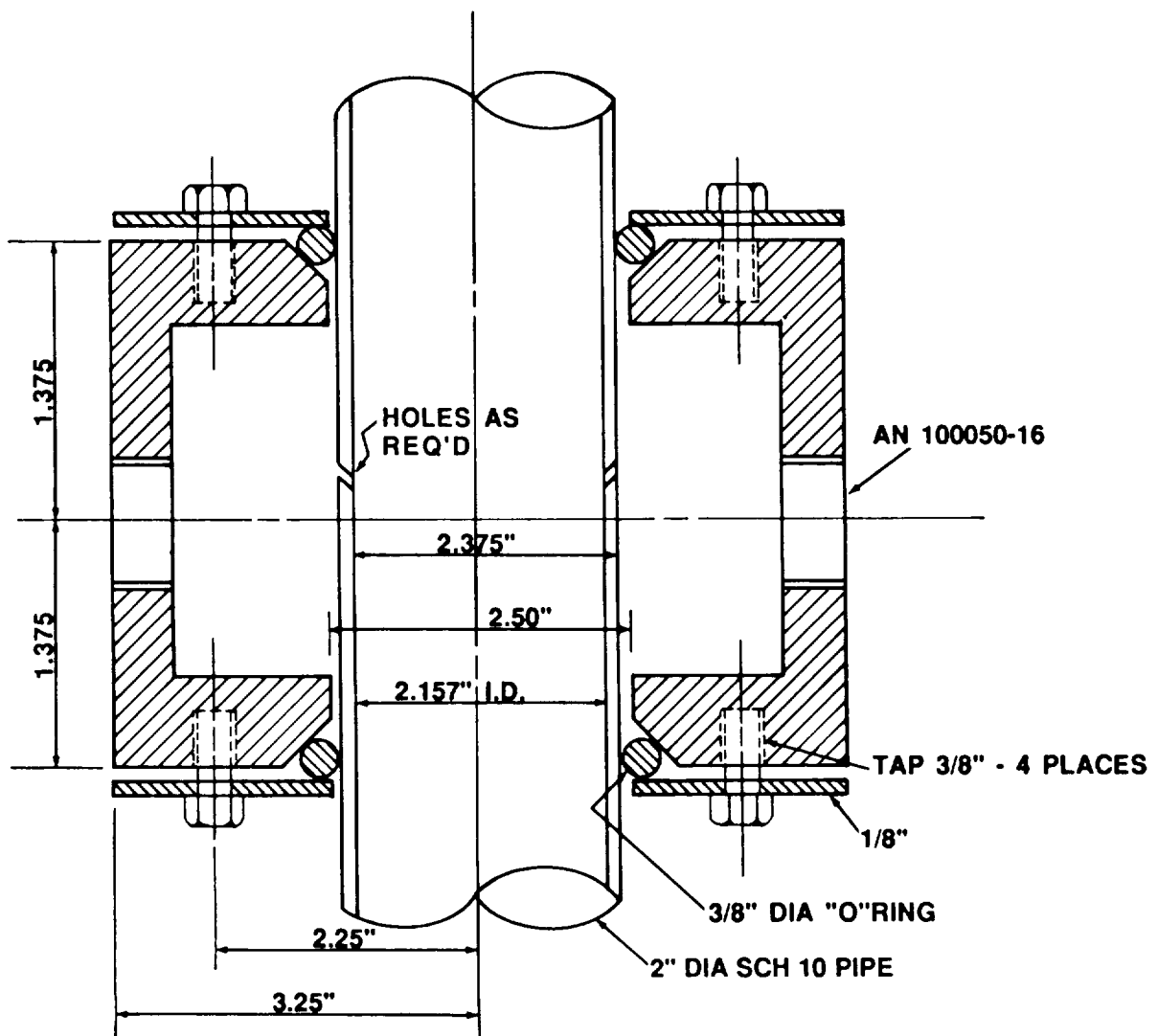


Figure 6. Drawing of water manifold.

DESCRIPTION

The dry tests were used to determine the basic mechanisms that influenced ignition overpressure. Table 1 shows the peak overpressure values for measurements K2 to K11 and the chamber pressure, chamber pressure peak, and the root sum square (RSS) of chamber pressure and chamber pressure peak for the dry SRM tests. Figure 7 shows the two typical types of chamber pressure time histories that occurred among the SRM test firings. One chamber pressure time history has a small chamber pressure (Pc) peak or Pc overshoot while the second time history shows a large Pc peak. Because of the differences in the SRM characteristics shown in Figure 7, the dry tests were also used to find a relationship to normalize the water injection tests. This was done so a better representation of the data could be presented. The chamber pressure rise rate, chamber pressure, chamber pressure peak, and chamber pressure impulse were investigated to determine the influence of each on IOP production. Study results indicate that IOP for the 1 percent SRM is basically controlled by the chamber pressure peak and resultant steady state pressure with lesser dependence on the chamber pressure rise rate.

Figure 8 shows the relationship between IOP and chamber pressure rise rate. Because of the small times involved (total rise rate occurs in 10 ms) and small variances in the rise rates for the SRMs, a relationship between IOP and chamber pressure rise rate was difficult to determine. Figure 8 shows that IOP and chamber pressure rise rate are not closely correlated.

The effect of chamber pressure impulse on IOP was also examined and is shown in Figure 9. Impulse is defined as the integration of pressure as a function of time from zero to a specific time increment (ΔT). Overpressure versus impulse is plotted for ΔT s of 20, 30, 40, and 50 msec for each of the dry tests. While there appears to be some relationship between chamber pressure impulse and IOP, a better relationship is shown between chamber pressure (Pc) and chamber pressure peak (Pc peak).

TABLE 1. PEAK OVERPRESSURE READINGS FOR DRY SRM TESTS

MSID	Location (in.)	TEST NUMBER								
		2	3	4	5	6	7	22	23	
K2	6	-	-	-	65	41	21.5	16	19	
K3	9	63	-	-	69	43	24	19	23	
K4	12	-	-	-	46	50	28	20	24	
K5	18	38	-	-	62	45	27	21	23	
K6	24	-	-	-	57	48	28	18	23	
K7	30	42	-	-	57	43	27	20	21.5	
K8	36	-	-	-	52	41	24	26	19	
K9	48	47	65	36	54	44	27	19	24	
K10	60	-	-	-	51	38	24	19	20	
K11	120	34	57	31	49	34	24	12	8	
AVERAGE (K2-K11)		-	-	-	56.2	42.7	28	19	20.5	
CHAMBER PRESSURE		1200	1200	1000	1000	800	780	730	750	
Pc peak		1640	1920	1120	1450	1520	780	730	810	
RSS Pc & Pc peak		2032	2265	1501	1761	1718	1103	1050	1104	

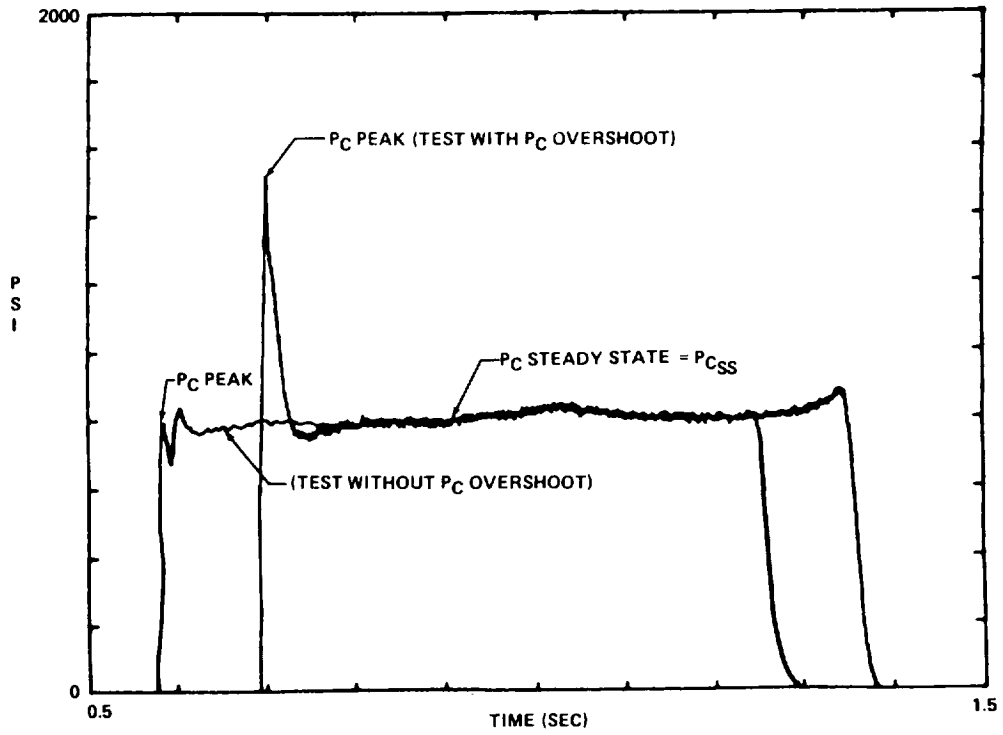


Figure 7. Typical chamber pressure time histories.

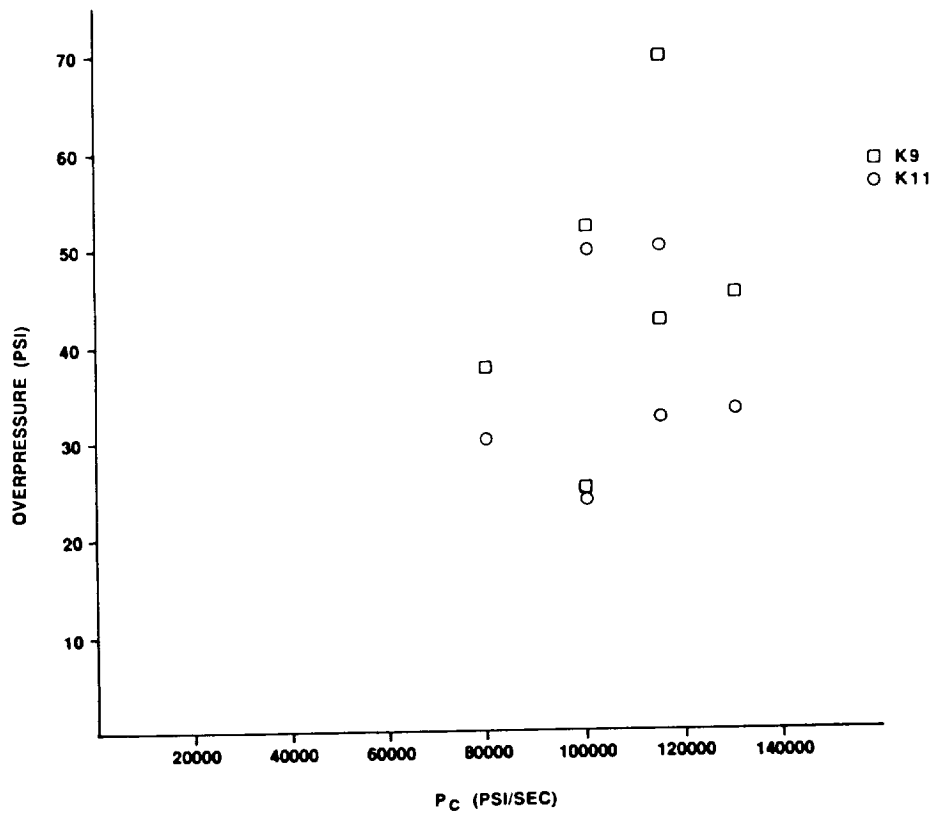


Figure 8. Overpressure versus chamber pressure rise rate.

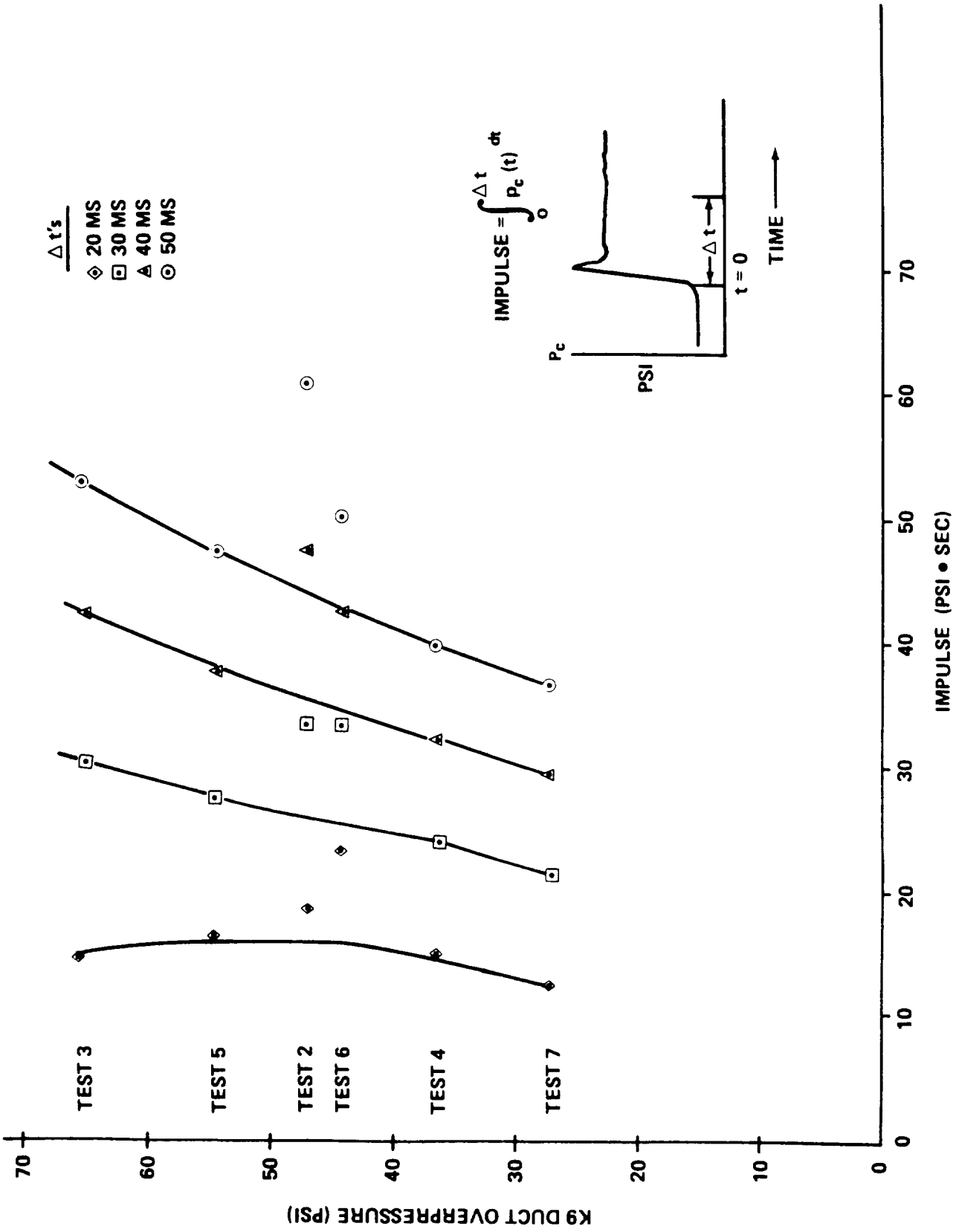


Figure 9. Duct overpressure measurement K9 versus chamber pressure impulse.

The relationship between IOP and Pc for pressure measurement K9 is shown in Figure 10. Figure 10 indicates that with an increase in chamber pressure an increase in overpressure occurs. While the figure shows a better correlation between IOP and Pc than between IOP and chamber pressure rise rate or chamber pressure impulse, an even better correlation is seen between IOP and Pc peak. Figure 11 shows the relationship between IOP and Pc peak for pressure measurements K9 for dry tests 2, 3, 4, 5, 6, 7, 22, and 23. This figure shows a linear relationship between IOP and Pc peak.

However, because it appears that both Pc and Pc peak are controlling factors in IOP, it was decided to use both in the normalizing relationship for the SRMs. This was done with a RSS of Pc and Pc peak. This relationship between IOP and the RSS of Pc and Pc peak was used to normalize the data from the water injection tests. Overpressure for pressure measurements K9 and K11 is plotted versus RSS of Pc and Pc peak in Figures 12 and 13. The figures show a near linear relationship between ignition overpressure and the RSS of Pc and Pc peak. A statistical analysis of the data gives a correlation coefficient value of 0.92 for measurement K9 and a correlation coefficient of 0.89 for measurement K11. Average duct overpressure (K2 to K11) versus RSS of Pc and Pc peak for dry tests 5, 6, 7, 22, and 23 is shown in Figure 14. Again, a linear relationship is shown between overpressure and the RSS of Pc and Pc peak. Using linear regression by method of least squares, the best fit is shown in Figure 14. The correlation coefficient for this data is 0.95. Figure 15 shows duct overpressure versus the RSS of Pc and Pc peak for the individual measurements K3, K6, K7, K8, K10, and K11 for tests 5, 6, 7, 22, and 23. For the tests with the lower normalization factor values, the pressure values of the individual measurements in the duct did not vary greatly. The figure does show that as the normalization factor increases the IOP value of each individual measurement also increases in a linear fashion. Also, the difference in pressure between each individual measurement increases as the RSS of Pc and Pc peak increases. Each pressure measurement K3, K6, K7, K8, K10, and K11 has a correlation coefficient of 0.89 or better. The average correlation coefficient for the five measurements is 0.94.

The next series of SRM firings were used to study water injection and foam as a means of reducing ignition overpressure. Table 2 shows the peak overpressure measurements, chamber pressure, chamber pressure peak, and the RSS of chamber pressure and chamber pressure peak for the water injection and foam tests. During the water injection tests, various flow rates were tested to try to establish a relationship between water flow rate and IOP reduction. Water injection tests were conducted using a water flow rate to propellant rate ratio ($\dot{\omega}_w/\dot{\omega}_p$) of 0.075, 0.15, 0.225, 0.3, 0.45, 0.6, 0.75, and 0.9. The physical test configuration could not accommodate flow rate ratios of 0.9 or higher. For the flow rate ratio of 0.9, the water exceeded the test configuration making the data for this flow rate invalid. An example of IOP reduction provided by water injection is shown in Figure 16. This figure shows time histories for pressure measurement K3 with water injection and without water injection. SRM firings were also conducted to test aerosol foam as a means of suppression. Duct overpressure versus distance from the nozzle exit plane for dry, foam, and water injection tests is plotted in Figure 17. This data has not been normalized to account for differences in motor characteristics of the different tests. The dry measurements plotted are an average of tests 4, 5, 6, 22, and 23. Figure 17 shows that all the water flow rates provided suppression of the IOP to some degree depending on the flow rate and duct location. The greatest suppression provided by the water injection was at pressure measurement K11 where the pressure wave exits the duct. The foam appears to cause an overall increase in the IOP. The foam did reduce the IOP exiting the duct slightly. Results indicate that because of the very low density of the foam, the volume of aerosol required would have to be very large relative to the source to provide greater suppression of the overpressure wave.

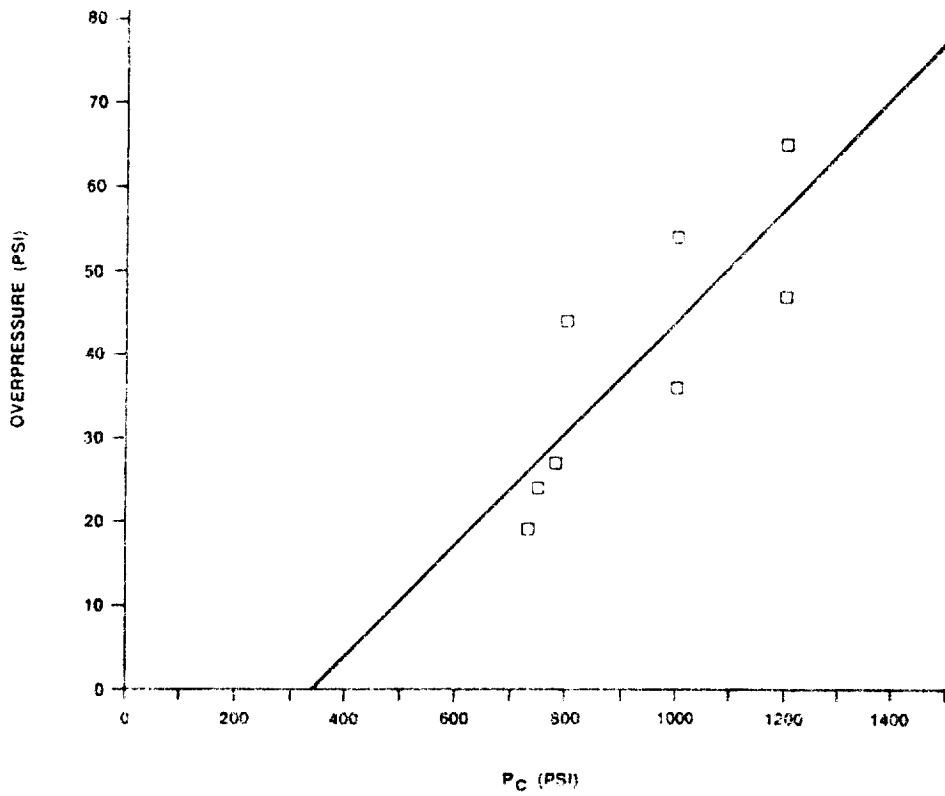


Figure 10. Overpressure (K9) versus chamber pressure.

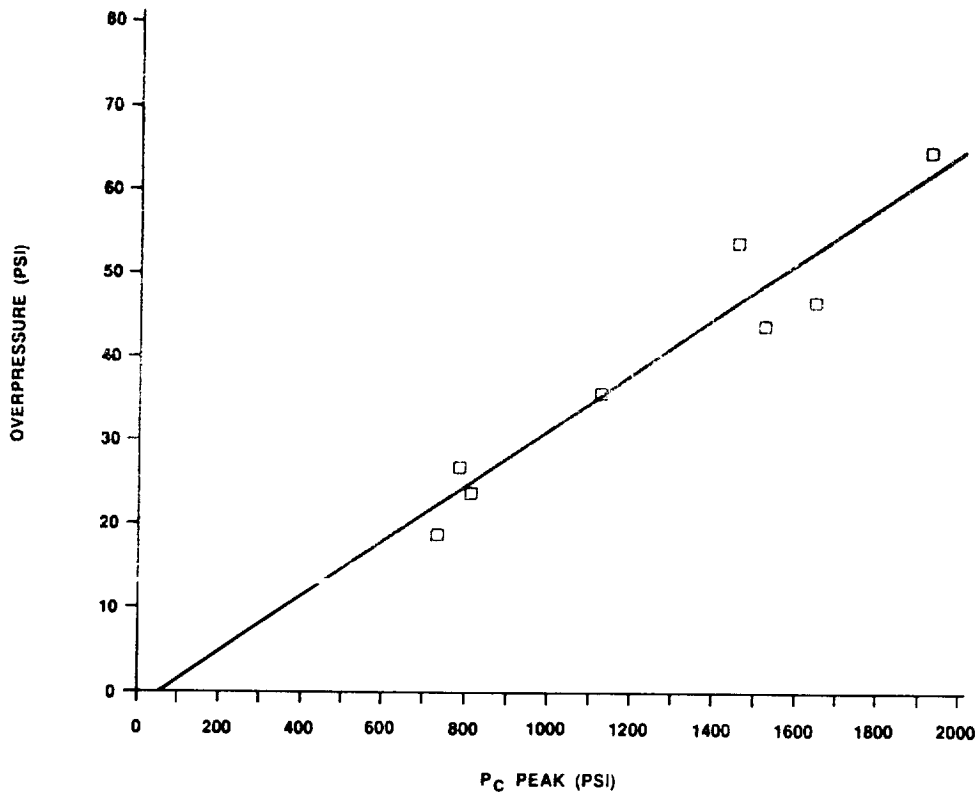


Figure 11. Overpressure (K9) versus chamber pressure peak.

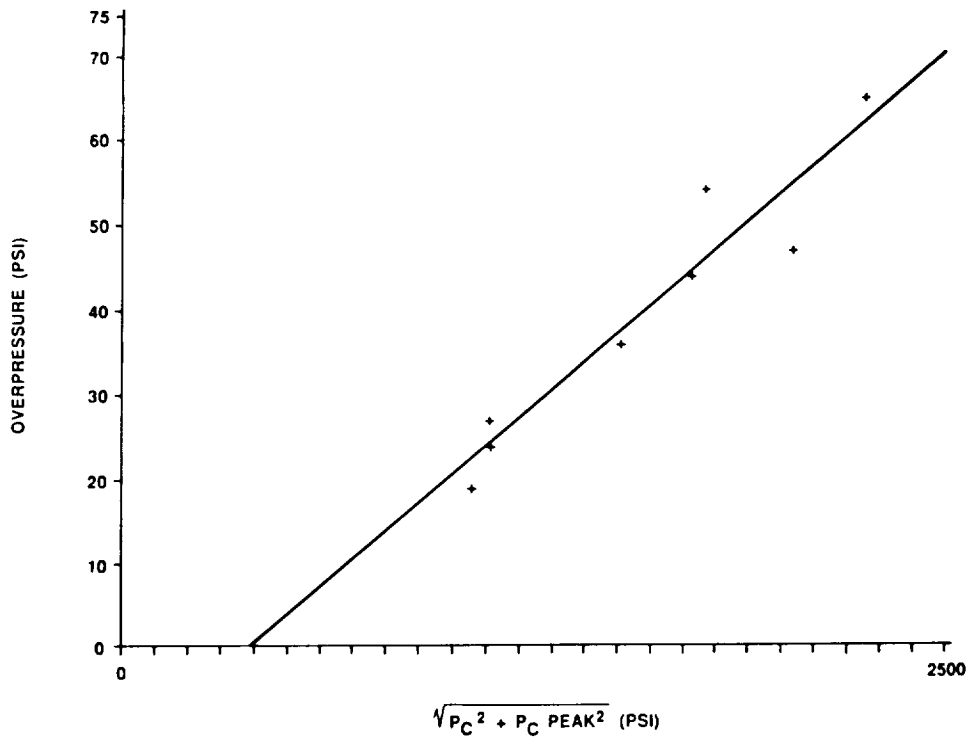


Figure 12. Overpressure (K9) versus RSS Pc and Pc peak.

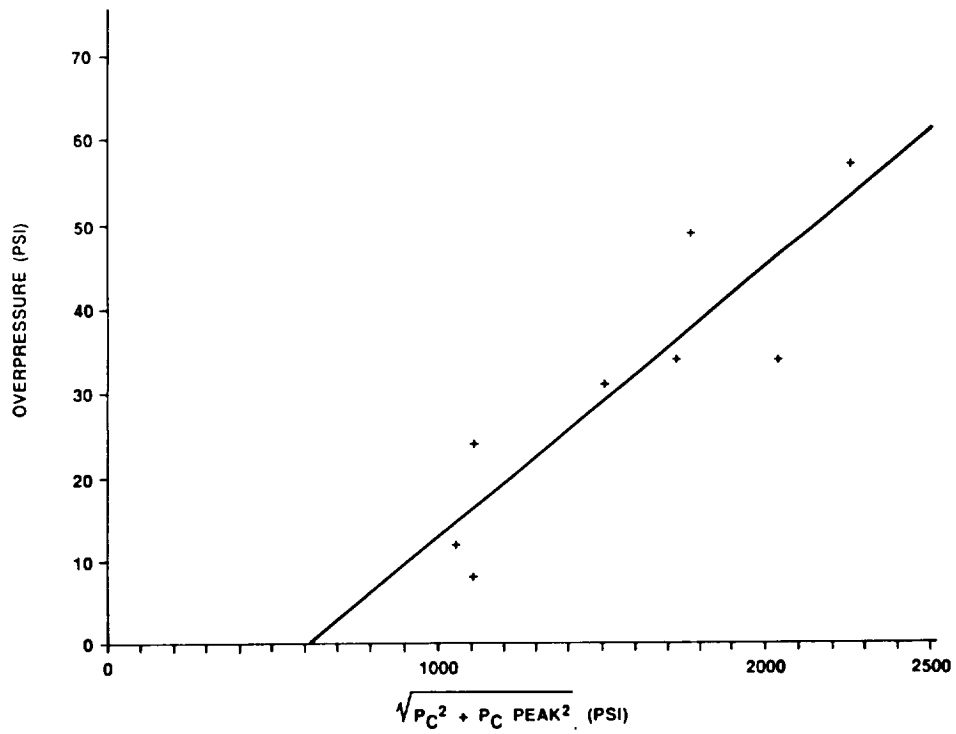


Figure 13. Overpressure (K11) versus RSS Pc and Pc peak.

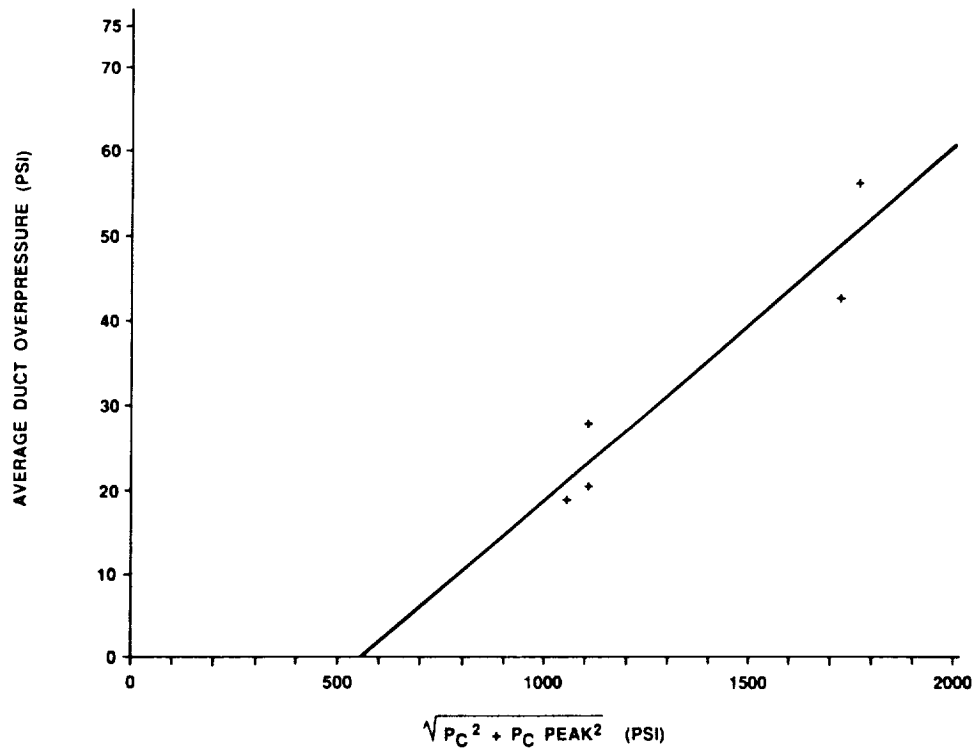


Figure 14. Average duct overpressure (K2-K11) versus RSS of Pc and Pc peak.

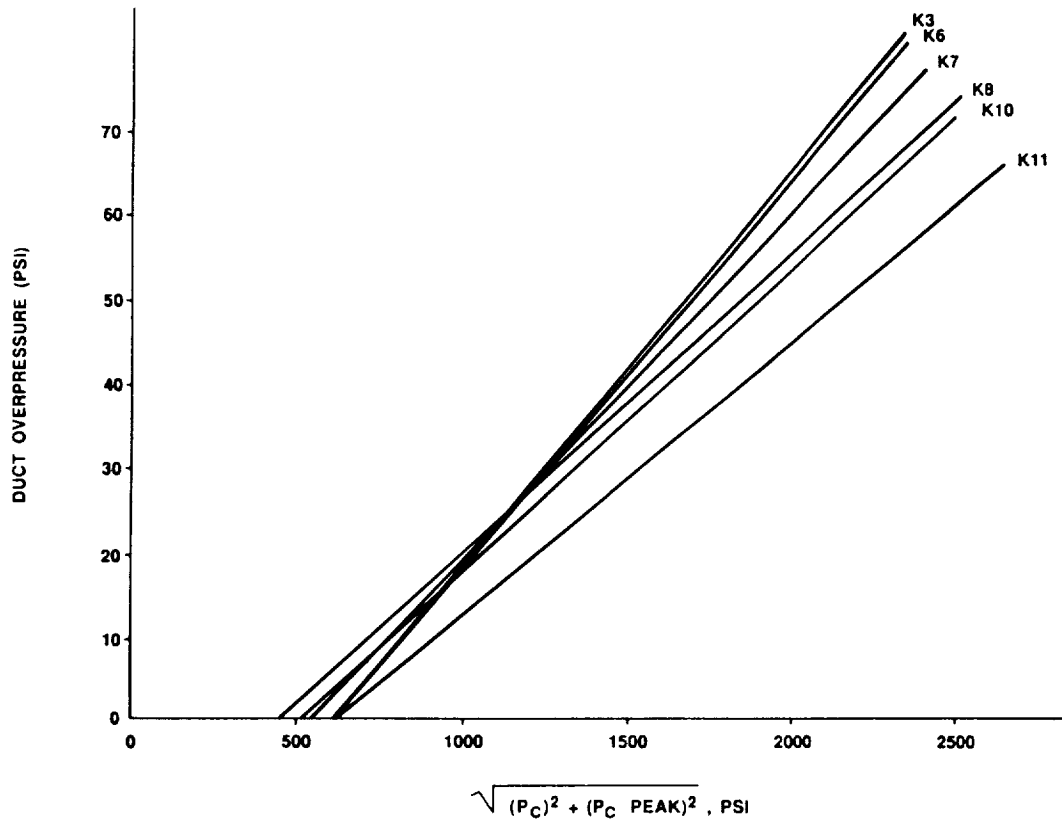


Figure 15. Duct overpressure (dry) versus RSS Pc and Pc peak.

TABLE 2. PEAK OVERPRESSURE READINGS FOR WET SRM TESTS

		Test Number												
		8	9	10	11	13	15	16	17	18	19	20	21	24
MSID	Location (in.)													
K2	6	10	13	43.5	40	45	24	25	21	11	20	34	25	10
K3	9	18	21	50	47.5	47	29	31	31	16	22	43	35	15
K4	12	20	19	45	48	44	29	31	26	19	23	44	32	15.75
K5	18	20	19.5	50	50	42	27.5	32	28	21	23	41	24	15.5
K6	24	23	22	46.5	49	42.5	27	35	48	22	24	42	23	17.5
K7	30	24	21.5	48.5	51	36.5	25	32	33	20	22	40	20	15
K8	36	22.5	22	45	50	35	22.5	33	38	19	21.5	40	20	15.25
K9	48	19	18	44	47.5	31	18	29	22	18	21	43	25	14
K10	60	19	17	44	47.5	27	16	25	21	12	21	35	20	14.5
K11	120	5	5	25	22.5	5	3.5	10	6	4	7.5	13	7	4.5
AVERAGE (K2-K11)		18	17.8	44	45	31.25	22.15	28.3	26.4	16.2	20.5	37.5	23.1	13.7
CHAMBER PRESSURE		825	810	850	850	830	800	835	800	800	825	825	825	790
Pc peak		650	730	700	675	1629	1460	1080	650	820	750	900	400	740
RSS Pc & Pc peak		1050	1090	1101	1085	1828	1665	1365	1030	1146	1115	1231	917	1032
Flow Rate Ratio		0.6	0.6	Foam	Foam	0.3	0.15	0.9	0.6	0.08	0.45	0.75	0.6	0.225

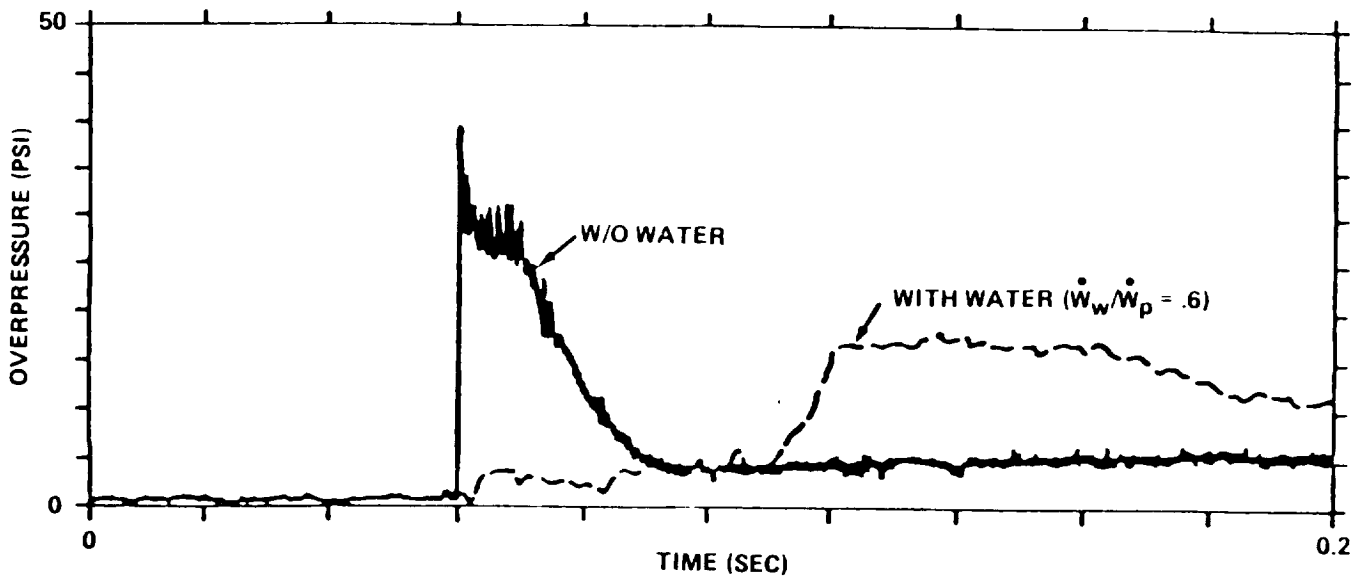


Figure 16. 1 percent SRM ignition overpressure test (with and without water injection).

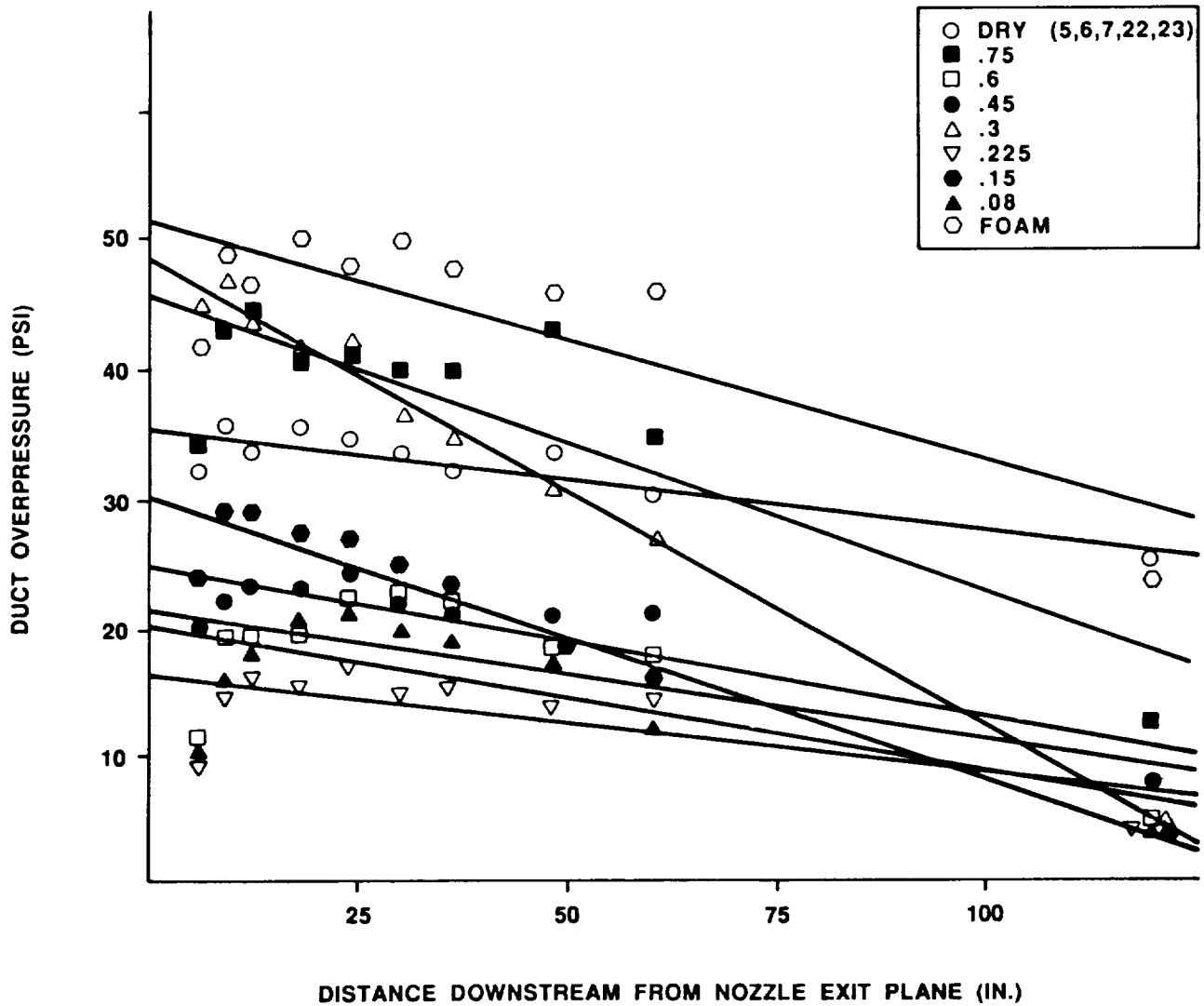


Figure 17. Unnormalized duct overpressure versus downstream location.

Figure 18 shows the normalized overpressure with water ratioed to dry overpressure (P_{water}/P_{dry}) plotted versus distance downstream. The flow rate ratios of 0.15, 0.225, 0.3, 0.6, and 0.75 are shown in the figure. The flow rate ratio of 0.15 provided the best suppression of the duct overpressure wave, reducing the IOP 1.5 to 10 times depending on the duct location. Figure 18 also shows that as the water flow rate increases the suppression of the overpressure decreases. The flow rate ratio of 0.6 provided very little suppression early in the duct. This can possibly be explained by the less efficient mixing of the water and exhaust that occurs with the higher water flow rates. The flow rate ratio of 0.75 did not reduce the overpressure wave except for measurement K11. In fact, the normalized data shows that the flow rate of 0.75 increased the IOP throughout the duct except for the last measurement.

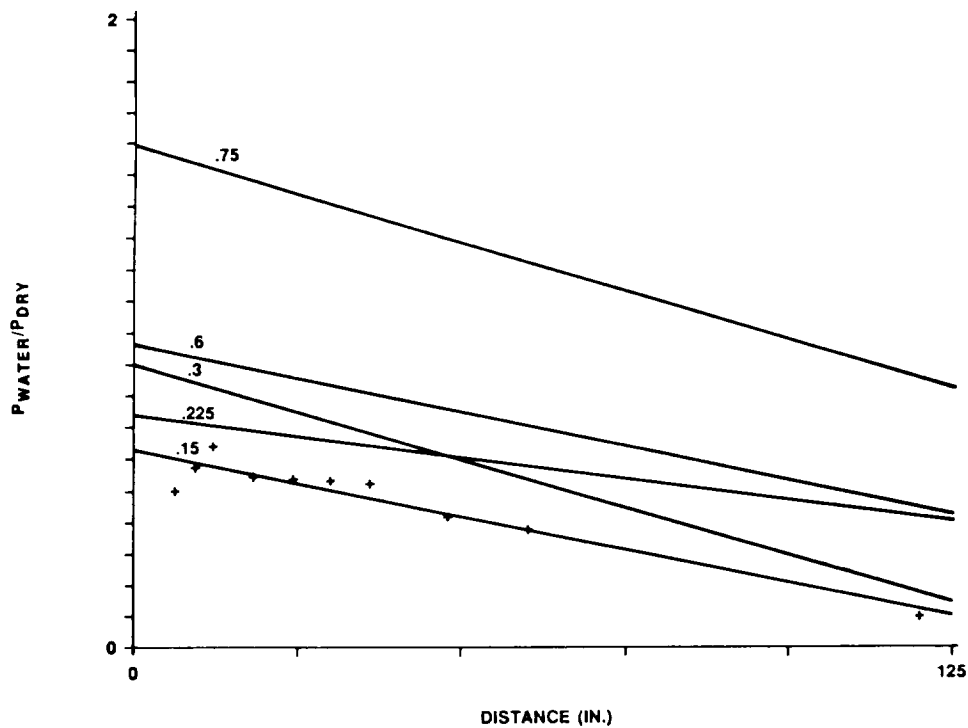


Figure 18. Normalized pressure ratio versus downstream location.

Figure 19 shows the downstream location versus overpressure wave arrival time of dry, foam, and water injection tests. The tests indicate that the higher the water flow rate the longer it takes the pressure wave to travel down the duct. The figure also shows that foam reduced the time it took the pressure wave to travel down the duct nine times or from 5 msec to 45 msec. For the water flow rate ratios of 0.6 and 0.9 the overpressure wave speed was greatly decreased after the downstream duct location of 60 in. Apparently with higher flow rate ratios, the mixing of the water and SRM exhaust gas is delayed and occurs at a later distance down the duct. Because the lower water flow rates (0.3, 0.225, 0.15) provided the best suppression of the IOP, but did not slow down the pressure wave as much as the higher flow rates, it can also be concluded that there is not a high correlation between reduction of the pressure wave speed to reduction of IOP.

Figure 20 shows the pressure ratio ($P_{\text{water}}/P_{\text{dry}}$) versus flow rate ratio for pressure measurements K7, K8, K9, K10, and K11. This figure indicates that the farther the pressure wave travels down the duct the greater the suppression provided by the water. This is true for all the water flow rates tested. This occurs because the exhaust gases from the SRM have more time to mix with the water and cool. The figure also shows that for each individual pressure measurement there appears to be a water flow rate range that provides the best suppression and as the water flow rate increases or decreases beyond this range the amount of IOP suppression decreases.

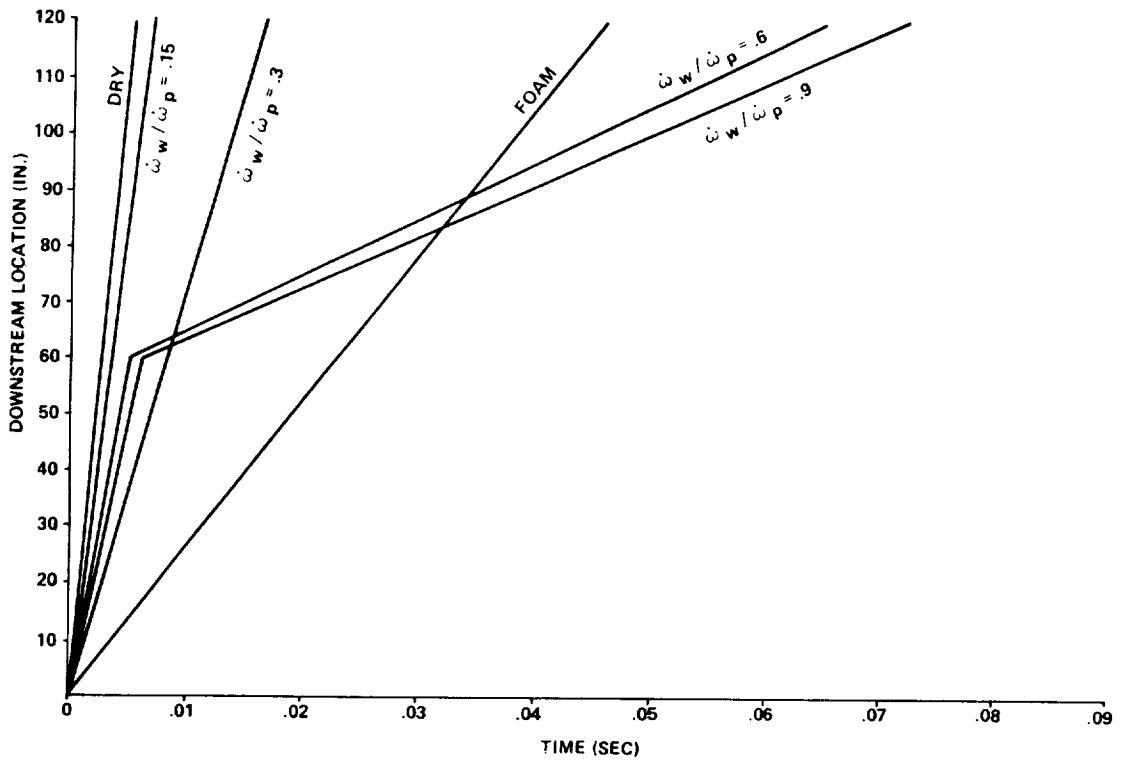


Figure 19. Downstream location versus overpressure wave arrival time.

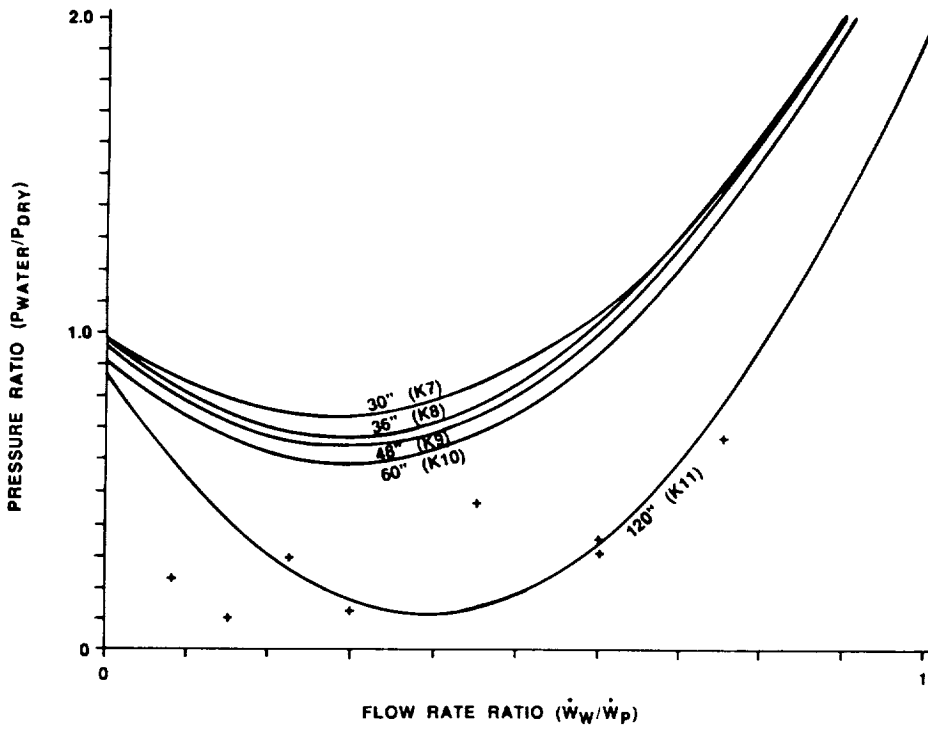


Figure 20. Normalized pressure ratio versus flow rate ratio.

Figure 21 shows the average normalized duct overpressure ratio ($P_{\text{water}}/P_{\text{dry}}$) versus flow rate ratio. $P_{\text{water}}/P_{\text{dry}}$ was averaged for pressure measurements K2 to K11. The best fit curve shown in Figure 18 was determined by the method of least squares assuming a parabolic relationship. The non-linear correlation coefficient is 0.90. The flow rate ratio of 0.225 provided the best suppression reducing the average duct overpressure by better than one-half. Figure 21 also indicates that there is an optimum range of water flow rates that provide the greatest suppression, and as this range is exceeded the effectiveness of the water injection system decreases. As the water flow rate increases beyond the optimum range, not only does the water no longer reduce the IOP, but it makes the overpressure worse. A possible cause for this increase in IOP is a choking of the flow which occurs when the water flow rate gets too high. With the higher flow rates not all the water is able to mix with SRM exhaust gases and the excess water is causing additional blockage of the flow.

Figure 22 shows the normalized exit pressure ratio versus flow rate ratio. The exit pressure ratio ($P_{\text{water}}/P_{\text{dry}}$) was normalized to the RSS of P_c and P_c peak. Assuming a parabolic relationship and using the method of least squares, the best fit curve is shown in Figure 22. The non-linear correlation coefficient for the data is 0.82. All the flow rate ratios provided significant reduction of the exit pressure wave, anywhere from 33 to 90 percent. The water flow rate to propellant flow rate ratio of 0.15 provided the best suppression. Again this data indicates that there is an optimum water flow rate range that gives the best suppression of the IOP. Figure 22 also indicates that as the amount of water used in the suppression system increases or decreased beyond the flow rate range of 0.15 to 0.6, the reduction of IOP significantly decreases.

The results of the 1 percent SRM water injection tests compare with previous 6.4 percent Shuttle Model Overpressure Tests (Eastern Test Range configuration) conducted at MSFC. The results of the 6.4 percent tests are shown in Figure 23 [2]. There are three major differences between the two tests: the 6.4 percent overpressure tests used SRMs scaled to 6.4 percent of the SRB; the 6.4 percent pressure measurements were made on a scaled Shuttle vehicle versus in the duct for the 1 percent tests; and the 6.4 percent SRMs were fired in an open exhaust duct system versus a closed duct used in the 1 percent SRM test firings. Despite these differences the results from the two tests are comparable. Both tests show that overpressure suppression to flow rate ratio is a parabolic function that has an optimum flow rate range that provides maximum suppression of IOP. Figure 23 also concurs with the conclusion that a decrease in suppression of IOP occurs as the water flow rate increases above the optimum range.

To find if IOP suppression could be improved by changing the location of the water injection system, additional SRM firings were conducted with the water injection system located at 20 and 40 in. away from the nozzle exit. The flow rate ratio used for these tests was 0.6. Figure 24 shows the normalized pressure ratio versus distance down the duct for the three different water injection system locations. Again the best fit of the data was found using the method of least squares. The effectiveness of water to suppress IOP was not improved by moving the water injection system further away from the nozzle exit. In fact, the test results indicate that the ability of water to suppress the IOP was decreased as the water injection system was moved further down the duct. Also, it appears when the water injection system was moved, the water acted as a wall and a pressure increase occurred above the point where the water injection system was located (Fig. 25). This figure shows that the IOP was increased more than two times above dry early in the duct when the water injection

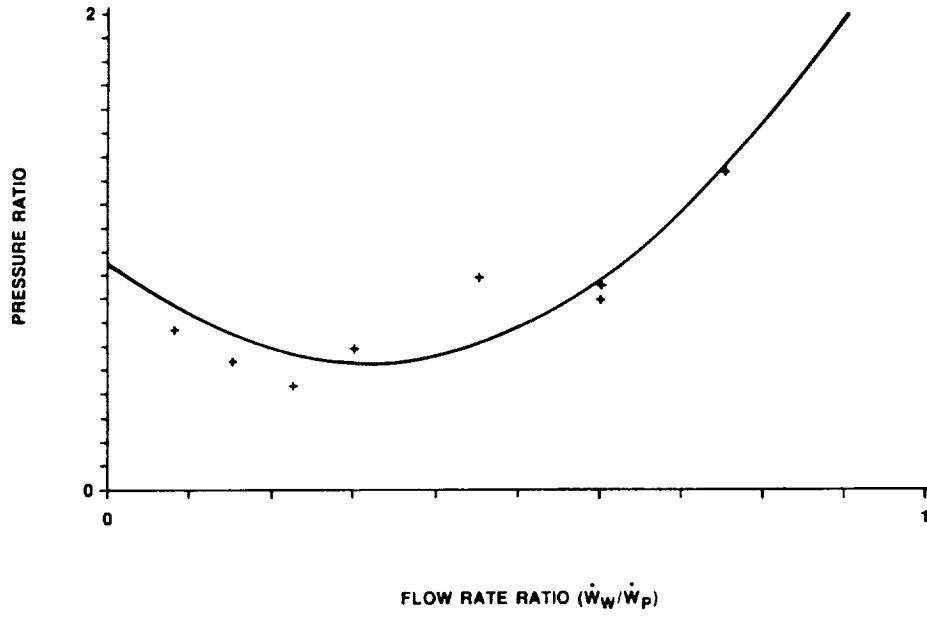


Figure 21. Average normalized pressure ratio versus flow rate ratio.

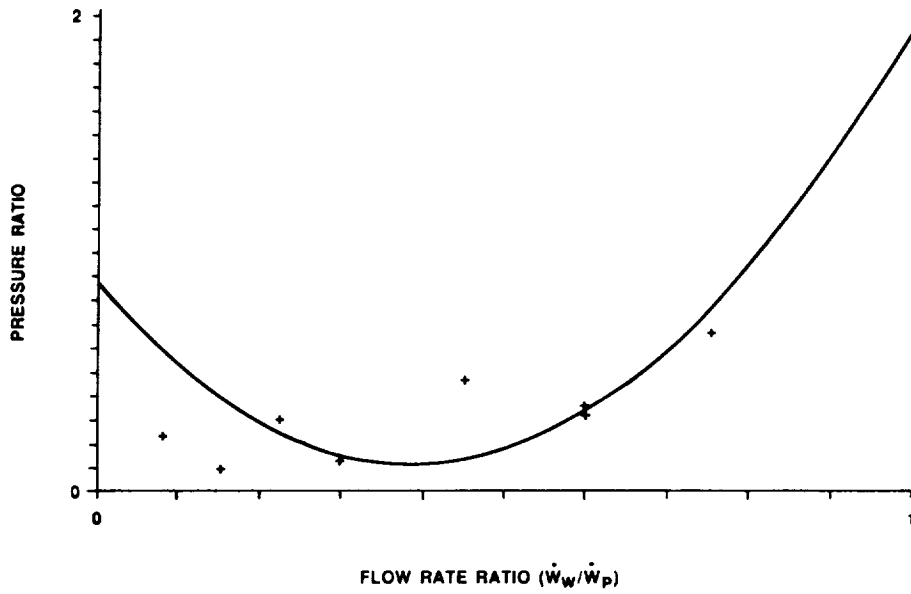


Figure 22. Exit pressure ratio (K11) versus flow rate ratio.

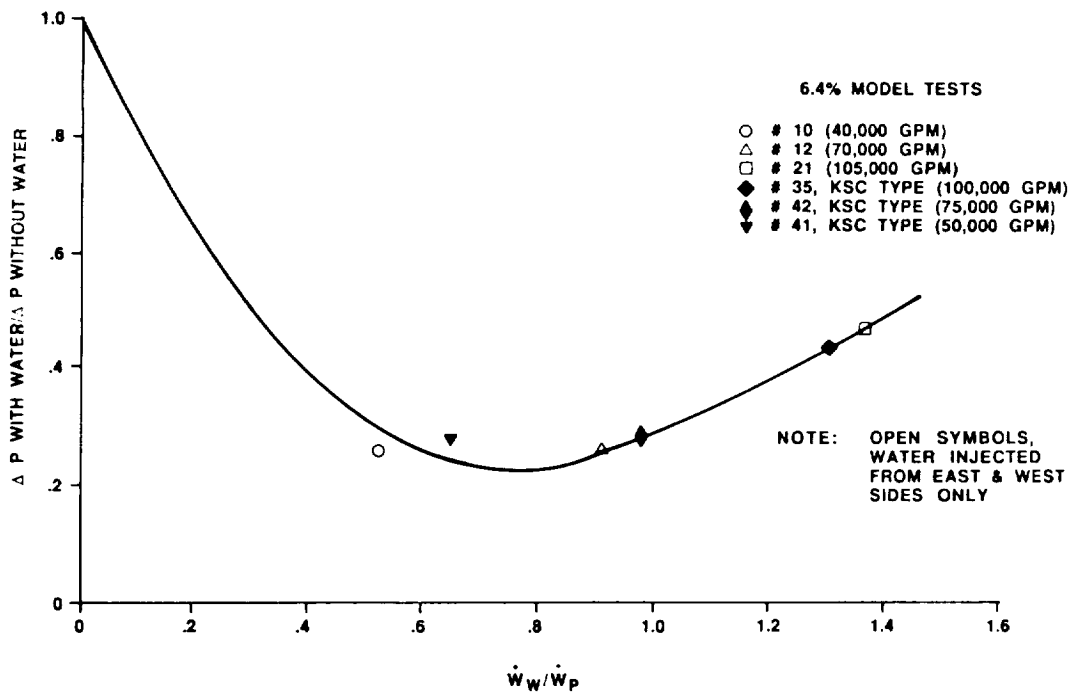


Figure 23. Pressure ratio for average vehicle measurements versus flow rate ratio (6.4 percent model tests).

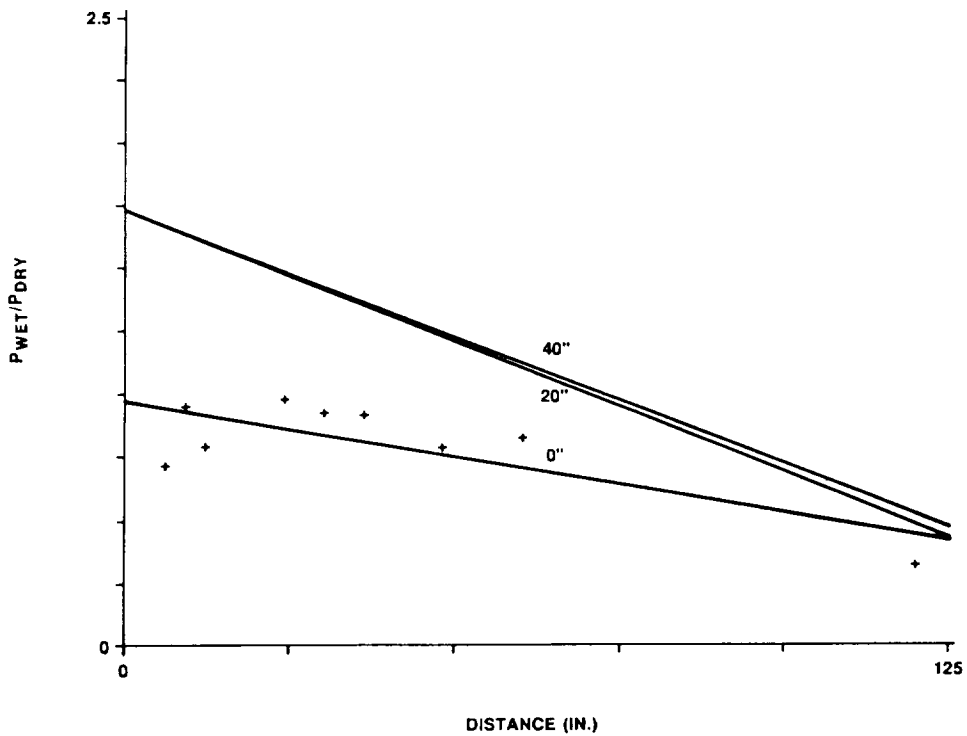


Figure 24. Pressure ratio versus downstream location (water injection system located at 0, 20, and 40 in. from nozzle exit plane).

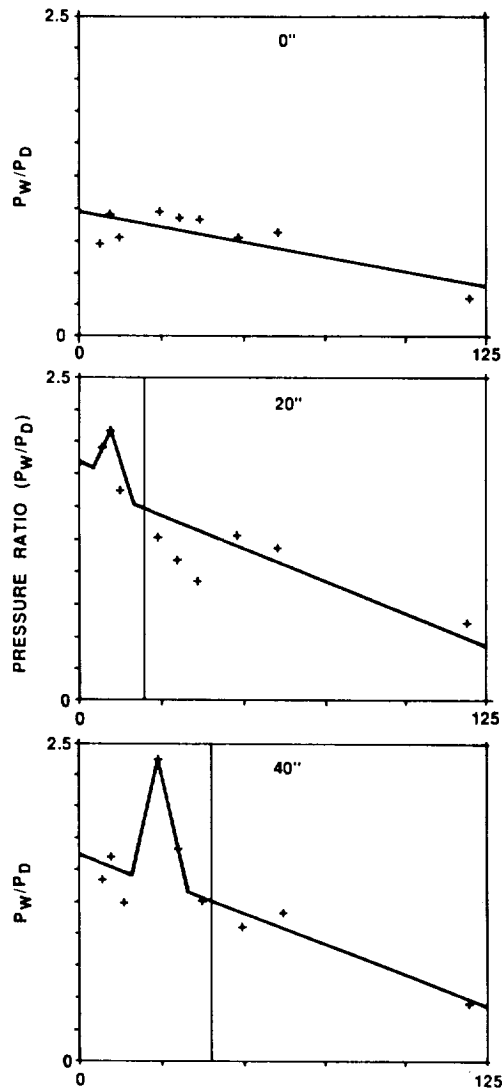


Figure 25. Normalized pressure ratio versus distance downstream.

system was located at 20 and 40 in. below the nozzle exit plane. However, the IOP exiting the duct was reduced in all three cases. The pressure exiting the duct was decreased by 42 percent when the injection system was located at 20 in., 54 percent when the injection system was located at 40 in., and 68 percent when the water injection system was located at the nozzle exit plane. The best suppression of the IOP exiting and throughout the duct occurred with the water injection system located at the nozzle exit plane.

CONCLUSIONS AND RECOMMENDATIONS

In conclusion, the basic mechanisms influencing IOP for the 1 percent SRM are chamber pressure and chamber pressure peak. It appears the chamber pressure rise rate would be a contributing factor only if P_c and P_c peak are the same for all motors. The results of the water injection tests indicate that a small amount of water is necessary to provide significant suppression. The lower flow rate ratios of 0.15, 0.225, and 0.3 provided the best suppression of the IOP. Furthermore, there is an optimum water flow rate range that is necessary to provide the best suppression. Also, as this range

is exceeded, the effectiveness of IOP suppression decreases and can cause an increase in the overall IOP as was the case with the higher flow rate ratio tested. Of the water injection system duct locations tested, the best suppression of the duct overpressure and exit overpressure occurred when the water injection system was located at the SRM nozzle exit plane. It can also be concluded from the study that reduction of the overpressure wave speed and IOP suppression are not closely correlated. Finally, while some suppression foam aerosol foam is seen, further testing of foam is necessary to determine its effectiveness as a means of suppressing IOP.

The utilization of the results obtained from this study have obvious potential impacts on large rocket launch facility design. There are other more subtle impacts that are not so obvious. For example, the decreased water flow rates for overpressure suppression in this study were found to be less than 20 percent of the total propellant flow rate as compared with a factor of more than four for the Western Test Range launch facility at VAFB. The not-so-obvious impacts include the exponential cost increases with large water tankage, piping, and valves for the higher flow rate system. The higher flow rate system yields a much cooler SRB exhaust temperature and gas solubility in liquid is inversely proportioned to temperature; thus, the cooler exhaust absorbs as much as seven times the hydrogen chlorine gas and results in higher acid concentrations in areas where waterborne droplets pass. The much greater flow rate systems also utilize a much greater quantity of water. The cost of procurement is obvious; the cost of properly treating (mechanically or chemically) every drop of recovered water and reusing the large volume results in an exponential cost factor versus the "brute force" water injection system.

These represent only one segment of the suppression issues, but the point is that research is mandatory to provide the optimum results, not only for the induced vehicle environment, but also for facility integration, cost, operational compatibility, and general system acceptance in terms of other interface disciplines.

Future work would include optimizing the suppression system. Other constituents could possibly be added to the water injected into the exhaust. These additives and how injected, how much, how effective, and how the system can be designed to decimate or greatly reduce the engineering and the total operating costs, are obvious factors for study. Related environments include thermal, acid fallout (HCL from SRM exhausts) and acoustics. Future work would include the integrated system evaluation for ignition overpressure.

REFERENCES

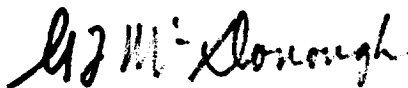
1. Dougherty, N. Sam; Nesman, Tomas E.; and Guest, Stanley H.: Shuttle SRB Ignition Overpressure. Model Suppression Test Program and Flight Results.
2. Jones, Jess H.: Scaling of Ignition Pressure Transients in Rocket Systems as Applied to the Space Shuttle Overpressure Phenomena. Presented at the 13th JANNAF Plume Technology Conference, NASA/JSC, March 1982.
3. Jones, Jess H.; and Guest, Stanley H.: Space Shuttle Ignition Overpressure Environments and Related Suppression Efforts. Presented at the Acoustical Society of America Meeting, Miami, FL., December 1981.

APPROVAL

IGNITION OVERPRESSURE STUDY FROM SOLID ROCKET MOTOR FIRINGS

By Douglas D. Counter

The information in this report has been reviewed for technical content. Review of any information concerning Department of Defense or nuclear energy activities or programs has been made by the MSFC Security Classification Officer. This report, in its entirety, has been determined to be unclassified.



G. F. McDONOUGH
Director, Structures and Dynamics Laboratory

